Suppoting information for

Two homochiral Eu^{III} and Sm^{III} enantiomeric pairs showing circularly polarized luminescence, photoluminescence and triboluminescence

Minghui Cui,[a] Ai-Ling Wang,[a] Cong-Li Gao,[a] Liming Zhou,[a] Tao Wu,*[b] Shaoming Fang[a] Hong-Ping Xiao,*[c] Feng-Cai Li and Xi-Li Li,*[a]

[a] Henan Provincial Key Laboratory of Surface and Interface Science, Zhengzhou University of Light Industry, Zhengzhou 450002, P. R. China; Email: lixl@zzuli.edu.cn

[b] Institute of Organic Chemistry and Biochemistry, Czech Academy of Sciences, Flemingovo náměstí 2, 16610 Prague 6, Czech Republic; Email: wu@uochb.cas.cz

[c] College of Chemistry & Material Engineering, Wenzhou University, Wenzhou 325035, P. R. China; Email: hp_xiao@126.com

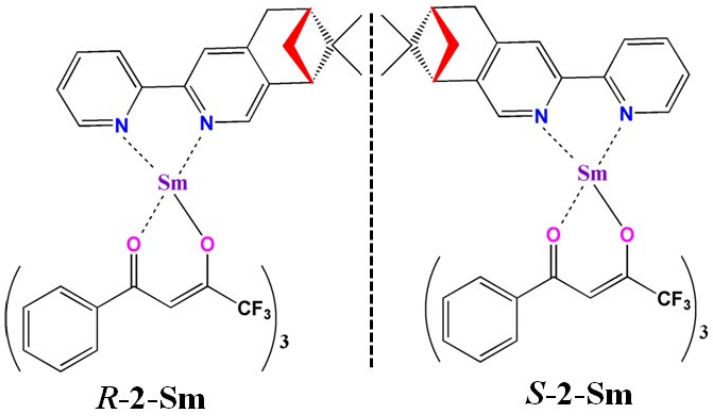

Scheme S1 Chemical structures of homochiral ***R*-2-Sm**/***S*-2-Sm**.

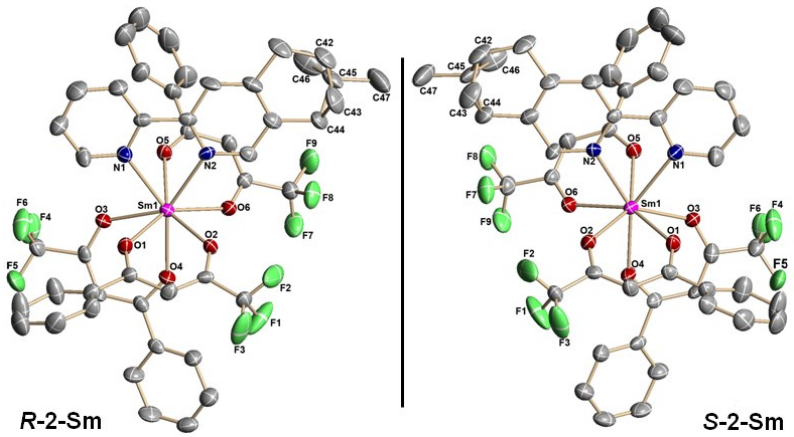

Fig. S1 Molecular structures of homochiral ***R*-2-Sm** and ***S*-2-Sm** enantiomeric pairs (ORTEP at 30% probability); H atoms are omitted for clarity.

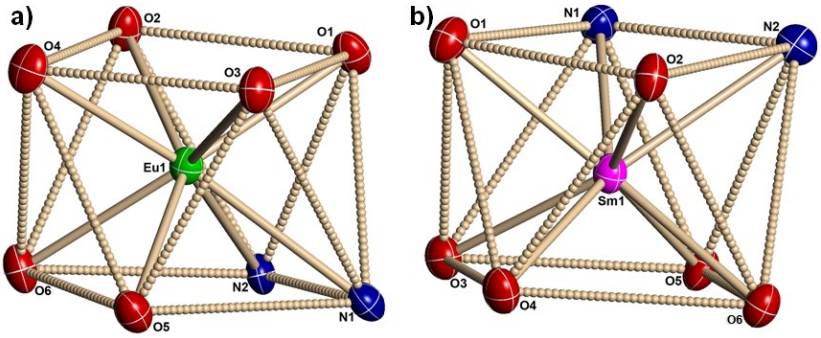

Fig. S2 Coordination geometries of Eu1 in ***R*-1-Eu** (a) and Sm1 in ***R*-2-Sm** (b).

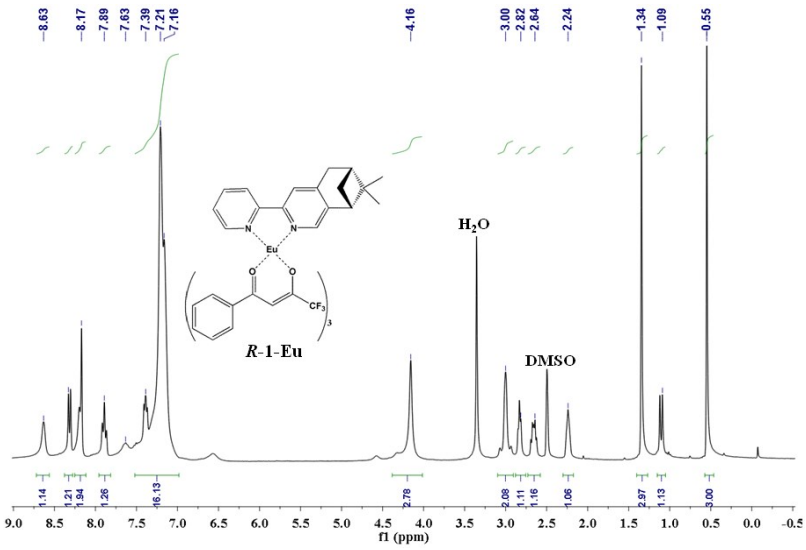

Fig. S3 ^{1}H NMR of ***R*-1-Eu** in DMSO-d_6. The NMR spectra for the homochiral Eu^{III} enantiomeric pairs are identical as expected.

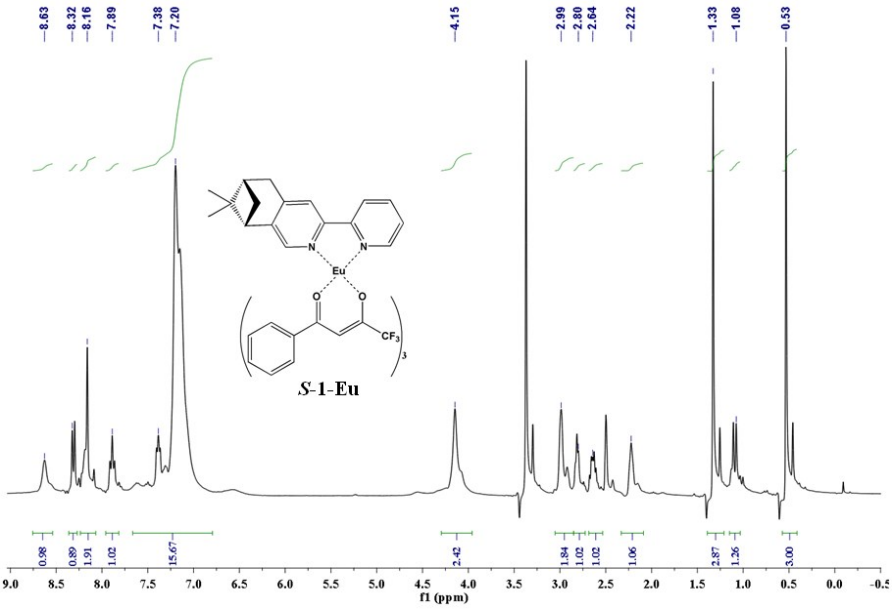

Fig. S4 ^{1}H NMR of ***S*-1-Eu** in DMSO-d_6. The NMR spectra for the homochiral Eu^{III} enantiomeric pairs are identical as expected.

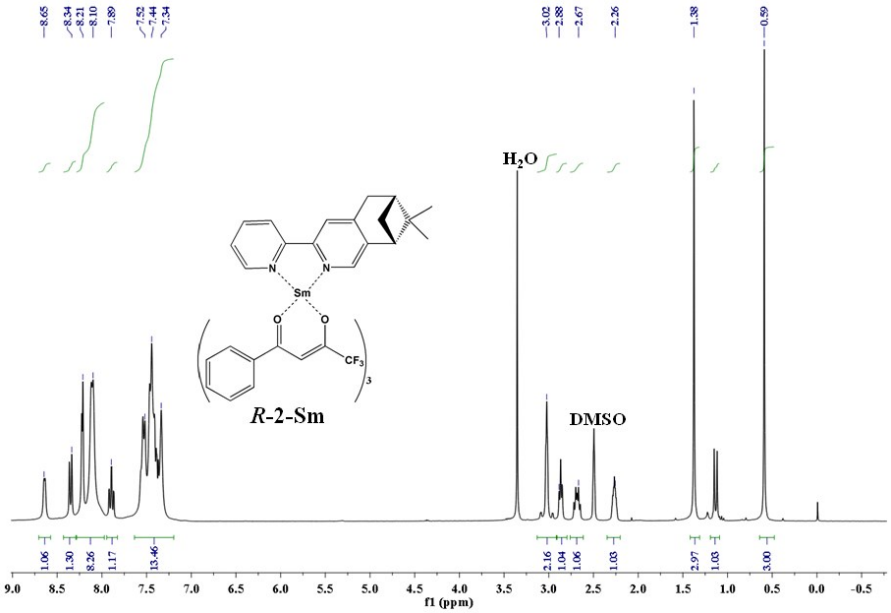

Fig. S5 ^{1}H NMR of ***R*-2-Sm** in DMSO-d_6. The NMR spectra for the homochiral Sm^{III} enantiomeric pairs are identical as expected.

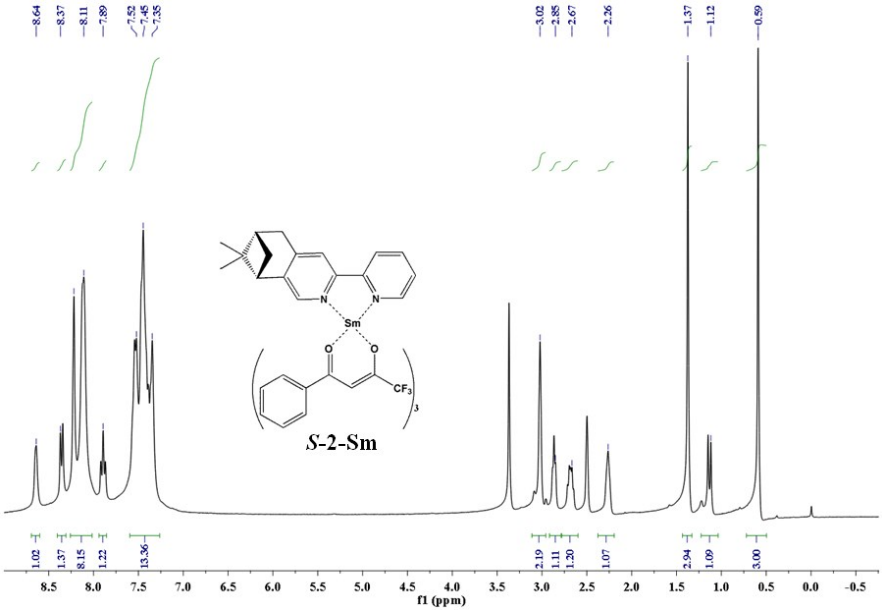

Fig. S6 ^{1}H NMR of ***S*-2-Sm** in DMSO-d_6. The NMR spectra for the homochiral Sm^{III} enantiomeric pairs are identical as expected.

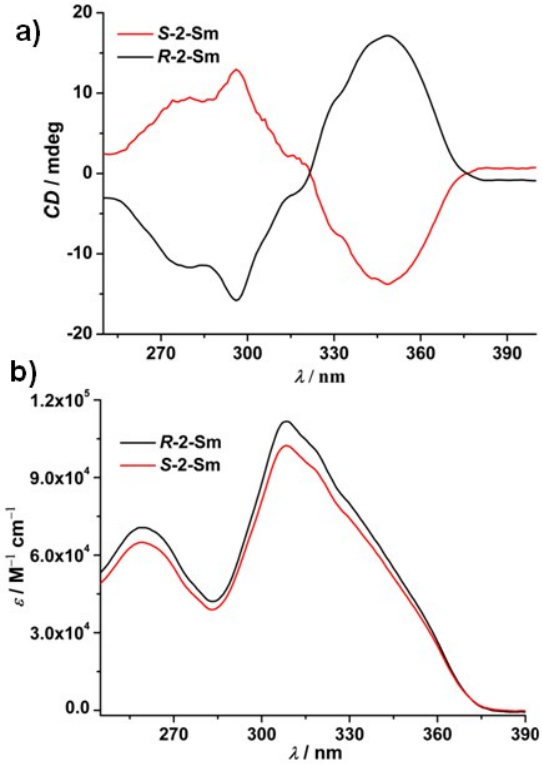

Fig. S7 (a) Electronic circular dichroism (ECD) spectra and (b) UV-Vis absorption spectra of homochiral ***R*-2-Sm** and ***S*-2-Sm** enantiomeric pairs in DCM (1×10^{-5} M).

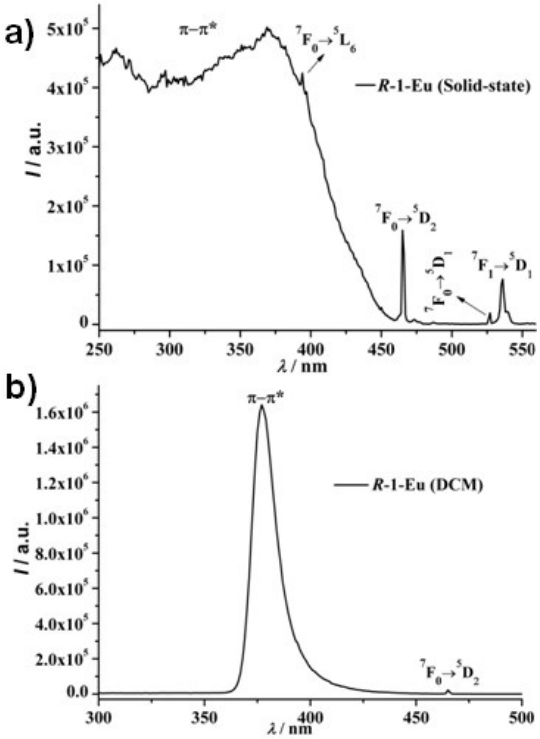

Fig. S8 The excitation spectra of ***R*-1-Eu** in the solid state (λ_{em} = 613 nm) (a) and in DCM (1×10^{-5} M, λ_{em} = 612 nm) (b).

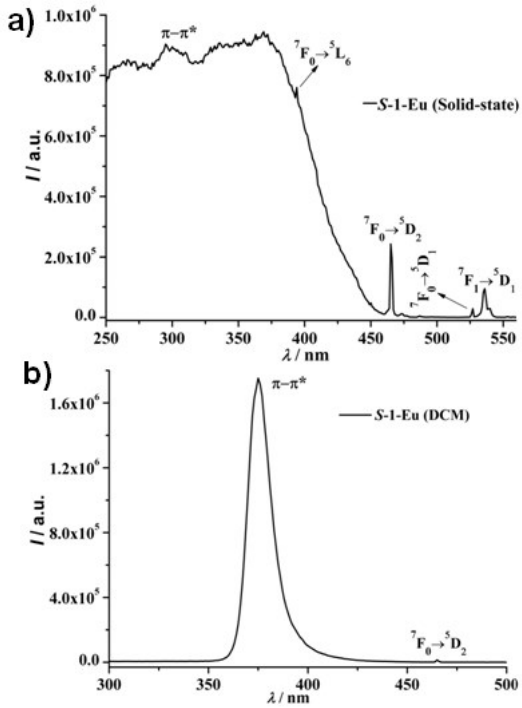

Fig. S9 The excitation spectra of ***S*-1-Eu** in the solid state (λ_{em} = 613 nm) (a) and in DCM (1×10^{-5} M, λ_{em} = 612 nm) (b).

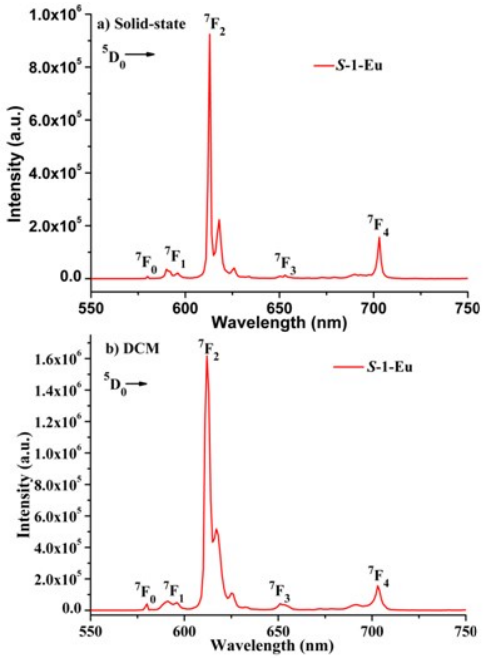

Fig. S10 Emission spectra of ***S*-1-Eu** in solid state (λ_{ex} = 370 nm) (a) and in DCM (1 × 10^{-5} M, λ_{ex} = 377 nm) (b) at room temperature.

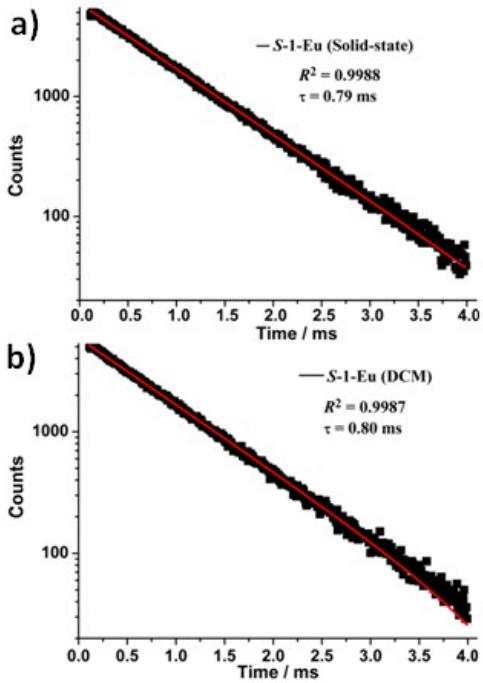

Fig. S11 Decay curves of ***S*-1-Eu** with fitted curves (red) in the solid state (a) and in DCM (1 × 10^{-5} M) (b) at room temperature. Decay curves presented with log ordinate scale.

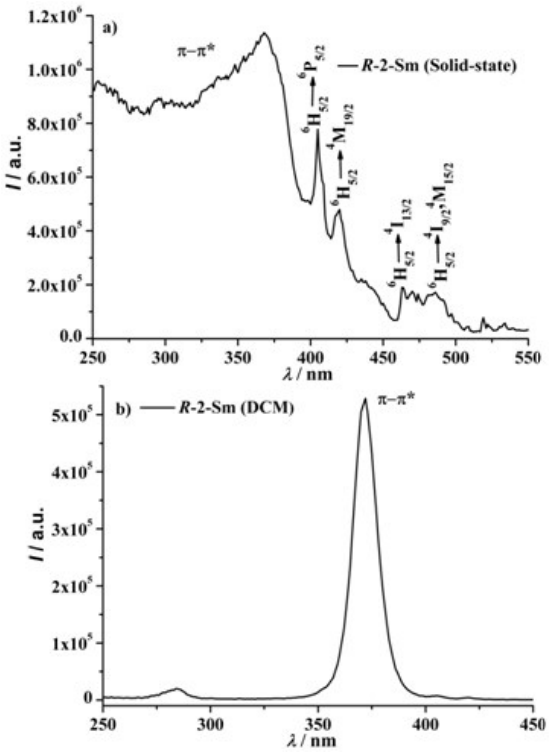

Fig. S12 The excitation spectra of ***R*-2-Sm** in the solid state (λ_{em} = 647 nm) (a) and in DCM (3×10^{-5} M, λ_{em} = 647 nm) (b).

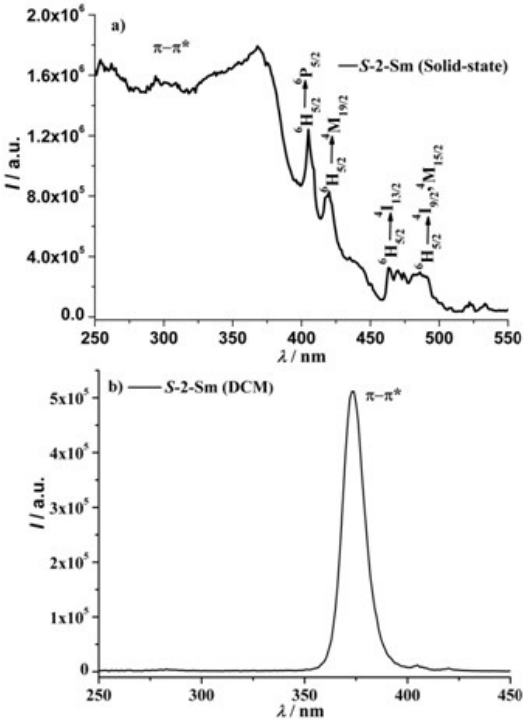

Fig. S13 The excitation spectra of ***S*-2-Sm** in the solid state (λ_{em} = 647 nm) (a) and in DCM (3×10^{-5} M, λ_{em} = 647 nm) (b).

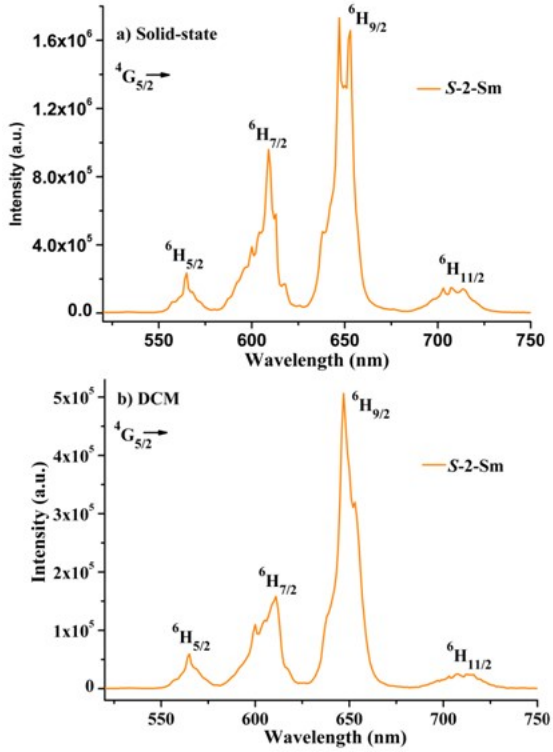

Fig. S14 Emission spectra of ***S*-2-Sm** in the solid state (λ_{ex} = 370 nm) (a) and in DCM (3×10^{-5} M, λ_{ex} = 370 nm) (b) at room temperature.

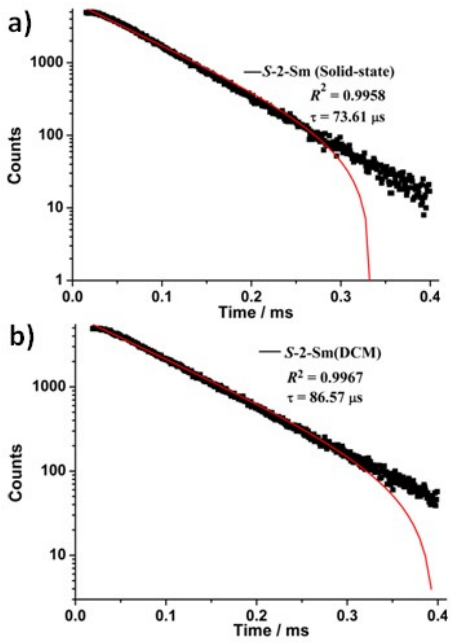

Fig. S15 Decay curves of ***S*-2-Sm** with fitted curves (red) in the solid state (a) and in DCM (3×10^{-5} M) (b) at room temperature. Decay curves presented with log ordinate scale.

Table S1 Crystallographic data and structure refinement parameters for both ***R*-1-Eu/ *S*-1-Eu** and ***R*-2-Sm/*S*-2-Sm** enantiomeric pairs.

	***R*-1-Eu**	***S*-1-Eu**	***R*-2-Sm**	***S*-2-Sm**
Chemical formula	$C_{47}H_{36}F_9N_2O_6Eu$	$C_{47}H_{36}F_9N_2O_6Eu$	$C_{47}H_{36}F_9N_2O_6Sm$	$C_{47}H_{36}F_9N_2O_6Sm$
Formula weight	1047.74	1047.74	1046.13	1046.13
Crystal system	triclinic	triclinic	triclinic	triclinic
Space group	*P*1	*P*1	*P*1	*P*1
a/Å	10.6976(9)	10.7349(3)	10.6922(7)	10.7328(4)
b/Å	10.7310(6)	10.7689(2)	10.7184(9)	10.7633(4)
c/Å	11.1962(9)	11.1509(4)	11.1514(8)	11.2076(4)
α/°	83.744(5)	83.873(2)	83.872(7)	83.741(3)
β/°	66.703(8)	66.744(3)	66.808(6)	66.691(4)
γ/°	73.668(6)	74.512(2)	74.017(7)	73.880(4)
V/Å^3	1132.85(16)	1141.33(6)	1129.30(16)	1142.29(8)
Z	1	1	1	1
D/g cm^{-3}	1.536	1.524	1.538	1.521
μ/mm^{-1}	1.471	1.460	1.387	1.371
GOF	1.000	0.965	1.038	1.023
$R_1{}^a$ /$wR_2{}^b$	0.0408 / 0.0892	0.0357 / 0.0708	0.0369 / 0.0770	0.0391 / 0.0718
Flack parameter	0.009(14)	0.0100(11)	0.014(10)	0.011(10)

^{a} $R_1 = \sum||Fo|-|Fc||/\sum|Fo|$. ^{b} $_wR_2 = [\sum w(Fo^2 - Fc^2)^2/\sum w(Fo^2)^2]^{1/2}$

Table S2. Selected bond lengths (Å) and angles (°) for ***R*-1-Eu** and ***S*-1-Eu**.

***R*-1-Eu**				***S*-1-Eu**			
Bond lengths (Å)		Bond angles (°)		Bond lengths (Å)		Bond angles (°)	
Eu1–N1	2.560(9)	O1–Eu1–N1	73.8(2)	Eu1–N1	2.626(6)	O2–Eu1–N2	80.72(18)
Eu1–N2	2.586(7)	O1–Eu1–N2	76.1(2)	Eu1–N2	2.625(6)	O2–Eu1–N1	132.96(18)
Eu1–O1	2.362(6)	O1–Eu1–O2	71.1(2)	Eu1–O1	2.415(5)	O2–Eu1–O1	70.19(17)
Eu1–O2	2.362(6)	O5–Eu1–N1	74.0(3)	Eu1–O2	2.402(5)	O6–Eu1–N2	76.34(18)
Eu1–O3	2.359(6)	O6–Eu1–O5	71.4(2)	Eu1–O3	2.396(5)	O5–Eu1–O6	70.75(17)
Eu1–O4	2.359(7)	N1–Eu1–N2	62.1(2)	Eu1–O4	2.407(5)	N1–Eu1–N2	61.3(2)
Eu1–O5	2.374(7)			Eu1–O5	2.416(5)		
Eu1–O6	2.344(6)			Eu1–O6	2.385(5)		

Table S3. Selected bond lengths (Å) and angles (°) for ***R*-2-Sm** and ***S*-2-Sm**.

***R*-2-Sm**				***S*-2-Sm**			
Bond lengths (Å)		Bond angles (°)		Bond lengths (Å)		Bond angles (°)	
N1–Sm1	2.580(7)	O5–Sm1–N2	76.1(2)	N1–Sm1	2.602(7)	O5–Sm1–N1	73.3(2)
N2–Sm1	2.584(6)	O5–Sm1–N1	73.8(2)	N2–Sm1	2.602(7)	O5–Sm1–N2	76.06(19)
O1–Sm1	2.394(6)	O5–Sm1–O6	70.77(19)	O1–Sm1	2.393(6)	O5–Sm1–O3	77.85(18)
O2–Sm1	2.354(6)	O2–Sm1–O1	71.16(19)	O2–Sm1	2.365(5)	O1–Sm1–O2	71.47(19)
O3–Sm1	2.364(5)	O1–Sm1–N1	73.9(2)	O3–Sm1	2.373(5)	O2–Sm1–N2	75.37(19)
O4–Sm1	2.368(6)	N1–Sm1–N2	62.2(2)	O4–Sm1	2.379(6)	N1–Sm1–N2	62.0(2)
O5–Sm1	2.367(5)			O5–Sm1	2.379(5)		
O6–Sm1	2.382(5)			O6–Sm1	2.377(6)		

Table S4. Continuous Shape Measures calculation for Eu1 atom in ***R*-1-Eu**.

OP-8	1 D8h	Octagon
HPY-8	2 C7v	Heptagonal pyramid
HBPY-8	3 D6h	Hexagonal bipyramid
CU-8	4 Oh	Cube
SAPR-8	5 D4d	Square antiprism
TDD-8	6 D2d	Triangular dodecahedron
JGBF-8	7 D2d	Johnson gyrobifastigium J26
JETBPY-8	8 D3h	Johnson elongated triangular bipyramid J14
JBTPR-8	9 C2v	Biaugmented trigonal prism J50
BTPR-8	10 C2v	Biaugmented trigonal prism
JSD-8	11 D2d	Snub diphenoid J84
TT-8	12 Td	Triakis tetrahedron
ETBPY-8	13 D3h	Elongated trigonal bipyrami

Structure [ML8]	OP-8	HPY-8	HBPY-8	CU-8	**SAPR-8**	TDD-8	JGBF-8	JETBPY-8	JBTPR-8	BTPR-8	JSD-8	TT-8	ETBPY-8
ABOXIY,	29.936,	22.050,	16.156,	9.275,	**0.508**,	2.427,	16.426,	27.351,	3.021,	2.346,	5.583,	9.988,	23.197

Table S5. Continuous Shape Measures calculation for Sm1 atom in ***R*-2-Sm**

OP-8	1 D8h	Octagon
HPY-8	2 C7v	Heptagonal pyramid
HBPY-8	3 D6h	Hexagonal bipyramid
CU-8	4 Oh	Cube
SAPR-8	5 D4d	Square antiprism
TDD-8	6 D2d	Triangular dodecahedron
JGBF-8	7 D2d	Johnson gyrobifastigium J26
JETBPY-8	8 D3h	Johnson elongated triangular bipyramid J14
JBTPR-8	9 C2v	Biaugmented trigonal prism J50
BTPR-8	10 C2v	Biaugmented trigonal prism
JSD-8	11 D2d	Snub diphenoid J84
TT-8	12 Td	Triakis tetrahedron
ETBPY-8	13 D3h	Elongated trigonal bipyrami

Structure [ML8]	OP-8	HPY-8	HBPY-8	CU-8	**SAPR-8**	TDD-8	JGBF-8	JETBPY-8	JBTPR-8	BTPR-8	JSD-8	TT-8	ETBPY-8
ABOXIY,	29.909,	22.041,	16.225,	9.385,	**0.510**,	2.379,	16.398,	27.342,	2.937,	2.284,	5.456,	10.063,	23.130

Table S6 Corrected emission transition intensities[a] relative to $^5D_0 \rightarrow {}^7F_1$ of ***S*-1-Eu** in the solid state and in DCM solution at room temperature

Parameter	∫0−0	∫0−1	∫0−2	∫0−3	∫0−4	∫total
Solid state	0.07 (580) [0.41%]	1.00 (590)	13.22 (613) [77.58%]	0.34 (653) [2.00%]	2.41 (703) [14.14%]	17.04
DCM	0.13 (580) [0.63%]	1.00 (591)	17.31 (612) [84.03%]	0.56 (651) [2.72%]	1.60 (703) [7.77%]	20.60

Values in the parentheses are the barycenter (nm) of emission transition, while the values in the square brackets are relative intensity (%) of each transition. [a] Estimated errors, ±5%.

Table S7 Radiative (A_r) and nonradiative (A_{nr}) decay rates, observed luminescence lifetime (τ_{obs}), radiative lifetime (τ_{rad}), intrinsic quantum yield (ΦEu Eu), overall quantum yield (ΦL Eu) and sensitization efficiency (η_{sen}) values of ***S*-1-Eu** in the solid state and in DCM at room temperature

***S*-1-Eu**	A_r (s^{-1})	A_{nr} (s^{-1})	τ_{obs} (ms)	τ_{rad} (ms)	ΦEu Eu (%)	ΦL Eu (%)	η_{sen} (%)
Solid state	930	327	0.79	1.08	74	59	80
DCM	871	392	0.80	1.15	69	51	74

Estimated errors: A_r, ±5 s^{-1}; A_{nr}, ±5 s^{-1}; τ_{obs}, ±2%; τ_{rad}, ±10%; ΦL Eu, ±10%; ΦEu Eu, ±12%; η_{sen}, ±16%.